Electronic properties of quasiperiodic heterostructures

J. E. Zárate and V. R. Velasco
Instituto de Ciencia de Materiales, Consejo Superior de Investigaciones Cientificas, Cantoblanco, 28049 Madrid, Spain
(Received 9 August 2001; published 26 December 2001)

We study the electronic states of different GaAs-AlAs Fibonacci, Thue-Morse and Rudin-Shapiro quasiperiodic heterostructures grown along the [001] direction. We employ an empirical tight-binding Hamiltonian including spin-orbit coupling together with the surface Green-function matching method. We present results for different generations of the quasiperiodic heterostructures, formed by different building blocks. We compare these results with those of the constituent quantum wells and with those of heterostructures containing the same total number of GaAs and AlAs slabs after periodic repetition of the building blocks. The states in the energy regions near the conduction- and valence-band edges of GaAs do not exhibit any spectrum fragmentation. They show a strong localization of the local density of states in the GaAs layers, and they can be traced to the states of the isolated quantum wells.

DOI: 10.1103/PhysRevB.65.045304 PACS number(s): 73.21.−b

I. INTRODUCTION

Many studies have been devoted to the physical properties of quasiperiodic systems[1–31] in the last 15 years. This interest was originally motivated from the theoretical side by the prediction that these systems should manifest nonconventional electron and phonon states,[9,11,23,25] exhibiting energy spectra with a high fragmentation and fractal character.[7,17,24] From the experimental side the growth of Fibonacci[2,3] and Thue-Morse[4] multilayers has provided the practical realization of these systems. The electronic structure of the Fibonacci systems has been investigated mainly in the single-band tight-binding limit. In these studies it was found that the energy spectrum is self-similar, and the energy bands divide into three subbands, each of which further subdivides into three and so on,[13–16] thus producing a singular continuous spectrum,[21] which in the infinite limit reduces to a Cantor spectrum[17] with dense energy gaps everywhere.[7–10] More realistic studies were presented in Refs. 28–30 by using an empirical tight-binding (ETB) sp^3s^* Hamiltonian.[32] It was stated in these more realistic studies that the Fibonacci spectrum could only be observed, and not clearly, for some energy ranges and for wave vectors in the vicinity of the superlattice Γ point. It was found also that the lower conduction and higher valence bands exhibited a selective spatial localization in the thickest GaAs slabs forming the structure.

It is necessary to consider that in the theoretical and experimental works one does not study a full infinite quasiperiodic sequence S_∞, but reaches only up to some high, but finite generation S_N, after repeated application of the generating rule. It is then a reasonable assumption to expect that the systems for sufficiently high N will display the essential features of the ideal infinite sequence. Thus, one takes S_N as an acceptable numerical approximation. This raises the question of the boundary conditions at the extremes of the finite structure as discussed in Ref. 31. Another question to be considered is the way of building the constituent blocks or generators in the sequence. In Refs. 2 and 3 the A and B blocks forming the quasiperiodic sequence contained AlAs-GaAs layers with different thicknesses in A and B. In other studies[4] A and B blocks contain only one material. It is then necessary to study if these circumstances can have some influence on the electron states of finite quasiperiodic systems.

The need to study more complicated sequences than the Fibonacci one can be derived among other things from the fact that the Rudin-Shapiro sequence does not satisfy the conditions for the theorems given in Refs. 17 and 21, and therefore its spectrum can have other properties.

We study here the electron states near the edges of the valence and conduction bands in finite realizations of the Fibonacci, Thue-Morse, and Rudin-Shapiro sequences, described by an ETB Hamiltonian, such as, those employed in Refs. 29 and 30. We shall compare the results of the quasiperiodic heterostructures with those of the constituent isolated quantum wells and with those of heterostructures having the same total number of blocks than the quasiperiodic ones, but obtained by means of a periodic repetition of the building blocks.

In Sec. II we discuss briefly the theoretical model and the method of the calculation. The results for the Fibonacci heterostructures are presented in Sec. III. Section IV gives the results for the Thue-Morse heterostructures and Sec. V presents the results for the Rudin-Shapiro heterostructures. Conclusions are presented in Sec. VI.

II. THEORETICAL MODEL AND METHOD OF CALCULATION

We use an ETB sp^3s^* Hamiltonian[32] including nearest-neighbor interactions and spin-orbit coupling.[33] The ETB parameters for AlAs are those employed in Ref. 34, and the ETB parameters for GaAs are those of Ref. 35. We have employed the following energy reference: $E_V(\mathrm{AlAs}) = -0.55$, $E_V(\mathrm{GaAs}) = 0.0$ eV. This band offset is within experimentally accepted values for (001) interfaces[36] and corresponds to a $\frac{66}{34}$ band-offset rule.[37] We shall study the (Γ) point of the heterostructures as the most likely candidate to show the characteristics of the spectra of the quasiperiodic systems.[29,30]

The quasiperiodic heterostructures involve many inequivalent interfaces. We shall use a version of the surface

Green-function matching method,[38] specially adapted to deal with an arbitrary number N of inequivalent interfaces.[39] The eigenvalues are obtained from the peaks in the imaginary part of the trace of the interface projection of the Green function of the matched system $\tilde{G}_S$.[39] A small imaginary part of 10^{-3} eV was added to the real energy variable, which was varied in steps of 0.005 eV (and for finer details in some areas in steps of 0.001 eV). The spatial localization was obtained by calculations of the local density of states (LDOS) in the different layers of the quasiperiodic heterostructures, which is directly obtained from the Green function of the whole system $\mathbf{G}_S$.[39]

III. FIBONACCI HETEROSTRUCTURES

The GaAs-AlAs Fibonacci heterostructures are grown by stacking recursively along the z direction, with two generators, blocks A and B, mapping the mathematical rule in the Fibonacci sequence

$$S_1=\{A\},S_2=\{AB\},S_3=\{ABA\},$$
$$S_4=\{ABAAB\},\ldots,S_n=S_{n-1}S_{n-2}. \quad (1)$$

In order to see the possible influence of the building blocks on the electronic structure of the finite Fibonacci generations we shall consider here two different A and B generating blocks. The first one, indicated by Fib I in the following, follows the scheme used in the experimental realization of a Fibonacci superlattice.[2,3] Thus we shall take an A block having 20 GaAs layers and 8 AlAs layers, and a B block having 10 GaAs layers and 8 AlAs layers. Our second choice, denoted by Fib II in the following, has an A block containing 20 GaAs layers and a B block containing 8 AlAs layers. In both cases the Fibonacci heterostructures will be sandwiched between semi-infinite AlAs slabs.

We present here results for the eight generation of the Fibonacci heterostructures, Fib I and Fib II, discussed above. The Fib-I eight generation contains 68 slabs of GaAs and AlAs layers, whereas the Fib-II eight generation contains 34 slabs of GaAs and AlAs layers. From Eq. (1) it is easy to see that Fib I will always have a repetition of the constituent 10 and 20 GaAs layers quantum wells. On the other hand Fib II, due to the presence of the *BAB* and *BAAB* subsequences, will have 20 and 40 GaAs layers quantum wells. In order to see the possible influence of the A and B building blocks on the electronic structure of the Fibonacci heterostructures, we shall study the electron states of the GaAs quantum wells having 10, 20, and 40 layers. As we have finite Fibonacci generations, it will be interesting also to compare the electronic structure of the Fibonacci heterostructures with those of the corresponding heterostructures having the same total number of slabs, but obtained by a finite periodic repetition of the *AB* sequence.

In Table I we present the lower conduction and higher valence-band states corresponding to AlAs-GaAs-AlAs quantum wells, having 10, 20, and 40 GaAs layers.

In Table II we present the corresponding electronic states for the Fib-I and Fib-II eight generations. It is easy to see, when looking to the results of Tables I and II, how the lower conduction states in the Fibonacci heterostructures have energies quite close to those of the corresponding single-quantum wells. The spatial confinement of those states in the corresponding GaAs slabs in the Fibonacci heterostructures is a clear signature of the origin of the states. The same is true for the higher valence-band states.

TABLE I. Energies (in eV) of the bound states near the GaAs valence-band top (negative values, VB) and the conduction-band bottom (positive values, CB) for (001) quantum wells as a function of n, the number of GaAs layers forming the well.

n	CB	VB
10		−0.051
		−0.115
20		−0.014
		−0.052
		−0.073
	1.634	−0.165
40		0.000
		−0.018
		−0.048
		−0.083
		−0.088
	1.659	−0.139
	1.551	−0.171

In order to see the spatial localization of the different electronic states in the Fibonacci generations we show in Fig. 1 the LDOS in the different layers of the Fib-II heterostructure and in 6 AlAs capping layers to the left and right of the Fib-II heterostructure, corresponding to the two lowest conduction-band states [(a) $E=1.555$, (b) $E=1.630$ eV]. In Fig. 1(a), the selective localization in the 40-layer GaAs wells can be seen. This is clearly seen eight times because of the presence of the *BAAB* subsequence 8 times in the Fi-

TABLE II. Energies (in eV) of the lower conduction states (CB) and higher valence (VB) states of the two types of eight generation Fibonacci heterostructures discussed in the text.

	CB	VB
Fib-I		−0.020
		−0.060
		−0.080
	1.700	−0.130
	1.630	−0.180
Fib-II		0.000
		−0.015
		−0.020
		−0.050
		−0.060
	1.695	−0.080
	1.655	−0.090
	1.630	−0.145
	1.555	−0.175

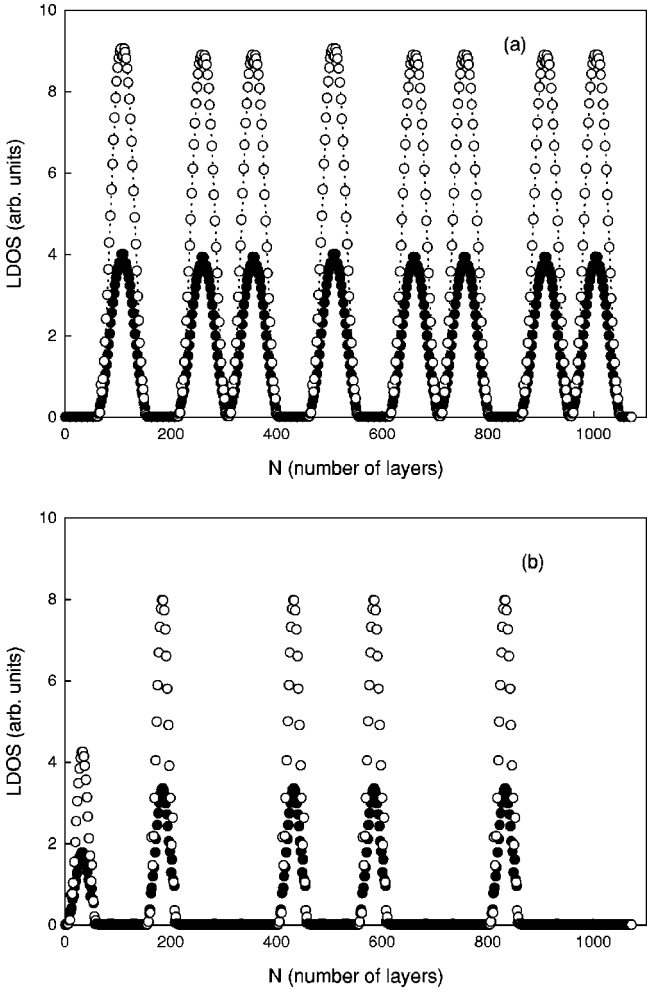

FIG. 1. Spatial distribution of the LDOS, in arbitrary units, of the two lowest conduction states at the Γ point in the different layers of a Fib-II eight generation Fibonacci heterostructure. (a) $E=1.555$; (b) $E=1.630$ eV. (●, anions; ○, cations).

bonacci sequence. Figure 1(b) shows the selective localization in the 20-layer-GaAs wells. We see five peaks corresponding to the existence of the *BAB* subsequence five times in the Fibonacci sequence.

In Fig. 2 we present the same information for the two highest valence band states [(a) $E=0.000$, (b) $E=-0.015$ eV]. The picture is the same as in Fig. 1. In Fig. 2(b) the spectral strength in the 40-layer GaAs wells is much lower than in the 20-layer wells although evident in the figure due to the existence of the second state of the 40-layer well close in energy to the present one.

In Table III we present the corresponding states for the periodic repetition 17 times of $(GaAs)_{20}(AlAs)_8$ and $(GaAs)_{20}(AlAs)_8(GaAs)_{10}(AlAs)_8$ blocks. It is easy to see when comparing Tables II and III that the energy values of the different states are quite similar, the only difference being the presence in the spectrum of Fib-II of the energy values corresponding to the 40-GaAs-layer quantum wells. For states having higher energy in the conduction-band region and lower energy in the valence-band region, it is possible to follow the analogy, although in some cases it is not so clear.

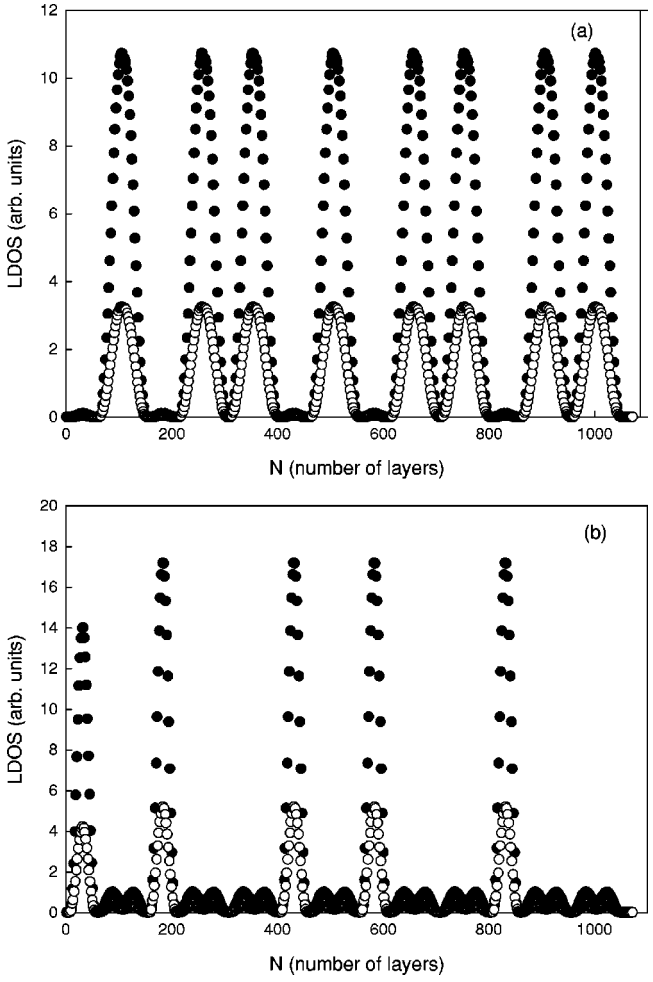

FIG. 2. Same as in Fig. 1 for the highest valence states. (a) $E=0.0$; (b) $E=-0.015$ eV.

We can see that it is not possible to distinguish the trifurcation of the Fibonacci spectrum in the cases considered here.

We have also studied the nineth generation of the Fib-II-type structure, including 55 AlAs and GaAs blocks, obtaining the same results discussed before for the eighth generation.

TABLE III. Energies (in eV) of the lower conduction-band (CB) and higher valence-band (VB) states of the periodic heterostructures formed by the periodic repetitions of the $(GaAs)_{20}(AlAs)_8$ [(20,8)] and $(GaAs)_{20}(AlAs)_8(GaAs)_{10}(AlAs)_8$ [(20,8,10,8)] blocks.

	CB	VB
(20,8)		−0.015
		−0.055
	1.697	−0.079
	1.630	−0.178
(20,8,10,8)		−0.016
		−0.058
		−0.079
	1.695	−0.132
	1.632	−0.179

TABLE IV. Energies (in eV) of the lower conduction (CB) and higher valence (VB) states of the two types of fifth and sixth generations complementary Thue-Morse heterostructures discussed in the text.

	CB	VB
TM-1		−0.015
		−0.060
		−0.080
	1.695	−0.135
	1.630	−0.175
TM-II		0.000
		−0.015
		−0.020
		−0.050
		−0.060
	1.695	−0.080
	1.655	−0.090
	1.630	−0.145
	1.555	−0.175

A Fib-II heterostructure having an *A* block containing 10 GaAs layers and a *B* block containing 8 AlAs layers, gives the same energy states as given by the Fib-I heterostructures studied before. This is because the *BAAB* subsequence gives 20-GaAs-layer wells in the heterostructure.

Similar results have been obtained in the case of $(GaAs)_{20}(AlAs)_8$ superlattices and superlattices having the seventh generation of the Fib-I system as period. It is then clear that in this case the results are independent of the different boundary conditions.

In Ref. 40 the electronic structure of a GaAs/AlAs Fibonacci superlattice with an enlarged well was studied by means of photoluminiscence spectroscopy. The structure was formed by two eighth generation Fib-I heterostructures with an extended well having two times the thickness of the well in the Fib-I structure. The system was symmetrical about the extended well and had two thick cladding AlAs layers. The photoluminiscence spectrum showed two peaks, one at $E \approx 1.58$ eV corresponding to the extended well and the second one at $E \approx 1.72$ eV corresponding to the Fibonacci heterostructure.

In order to check the results coming out from our calculations we have considered a similar structure but with two seventh generation Fib-I heterostructures instead of the eighth. We do so due to memory limitations in our computer. Our *A* block is formed by $(GaAs)_{20}(AlAs)_8$ and the *B* block by $(GaAs)_{20}(AlAs)_4$. The extended well is 40 GaAs layer thick. These data are quite close to the experimental system in Ref. 40. We have found for this heterostructure the two lowest conduction states at $E=1.555$ (localized in the 40-layer well) and at $E=1.630$ eV (localized in the 20-layer wells of the Fib-I structures). The two highest valence states are located at $E=0.0$ (localized in the 40-layer well) and at $E=-0.015$ eV (localized in the 20-layer wells of the Fib-I structures). Thus we should have a transition at $E=1.555$ eV corresponding to the enlarged well and a higher one at $E=1.645$ eV corresponding to the Fib-I heterostructures. These values, without excitonic corrections, agree reasonably well with those of Ref. 40.

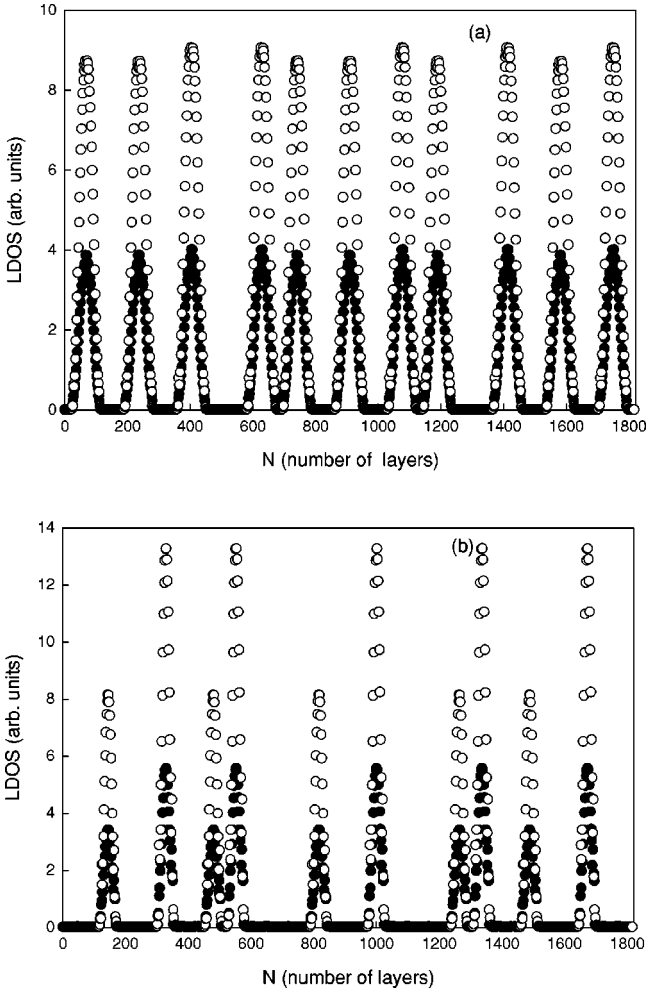

FIG. 3. Same as in Fig. 1 for the sixth generation of the complementary TM-II system.

IV. THUE-MORSE HETEROSTRUCTURES

These structures are produced by stacking recursively along the *z* direction, with two generators, blocks *A* and *B*, mapping the mathematical rule in the Thue-Morse sequence[41]

$$S_0=\{A\},S_1=\{AB\},S_2=\{ABBA\},\ldots,S_{n+1}=S_n\overline{S}_n, \quad (2)$$

$$\overline{S}_0=\{B\},\overline{S}_1=\{BA\},\overline{S}_2=\{BAAB\},\ldots,\overline{S}_{n+1}=\overline{S}_nS_n. \quad (3)$$

The $\overline{S}_n$ sequence is complementary to the S_n one, and the number of terms in the sequence goes as 2^n.

The same *A* and *B* blocks are considered as in the Fibonacci systems, for both I and II cases, that now we shall denote as TM I and TM II, respectively.

We present here results for the fifth generation of the Thue-Morse TM-I structure and the sixth generation of the TM-II structure. The TM-I fifth generation contains 64 slabs

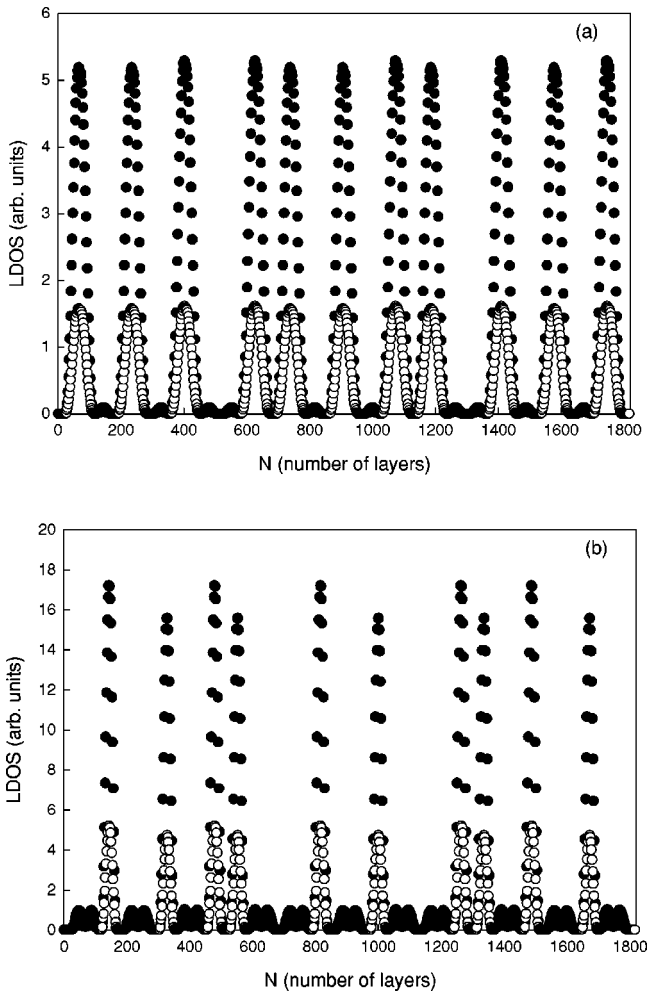

FIG. 4. Same as in Fig. 2 for the sixth generation of the complementary TM-II system.

of GaAs and AlAs layers, whereas the TM-I sixth generation also contains 64 slabs of GaAs and AlAs layers. The TM-I, as the Fib-I, structure will have always a repetition of the constituent 10- and 20-GaAs-layer quantum wells. On the other hand the TM-II structure, due to the presence of the *BAB* and *BAAB* subsequences, will have 20- and 40-GaAs-layer quantum wells.

In Table IV we present the lower conduction and higher valence states of the complementary TM-I fifth and TM-II sixth generations, respectively. It is easy to see that we obtain basically the same results shown in Table II for the Fibonacci heterostructures. The normal sequences give the same results presented here.

In Fig. 3 we present the LDOS corresponding to the two lowest conduction states, in the different layers of the complementary TM-II structure and in six neighboring AlAs layers to the right and left of the quasiperiodic heterostructure. In Fig. 3(a) we see the localization in the 40-layer-GaAs wells, appearing 11 times in the Thue-Morse sequence. In Fig. 3(b) the localization is seen in the 20-layer-GaAs wells appearing ten times in the structure. The behavior is completely analogous to that seen in the Fibonacci heterostructures.

TABLE V. As in Table I for the $n=8$, 30, 50, and 60 GaAs layers quantum wells.

n	CB	VB
8		−0.070
		−0.143
		−0.279
30		−0.004
		−0.029
		−0.034
		−0.082
	1.576	−0.125
50		0.002
		−0.010
		−0.030
		−0.058
	1.613	−0.092
	1.538	−0.127
60		0.003
		−0.006
		−0.020
		−0.039
	1.669	−0.043
	1.585	−0.064
	1.530	−0.094

In Fig. 4 we present the same information as in Fig. 3 for the two highest valence states. The picture is the same as seen in Fig. 3. In Fig. 4(b) we can also see the lower spectral strength in the 40-layer-GaAs wells coming from the second state of this well quite close in energy to the present one.

It is then clear that we obtain basically the same picture seen in the Fibonacci heterostructures.

TABLE VI. Energies (in eV) of the lower conduction (CB) and higher valence (VB) states of the two types of fifth and sixth generation Rudin-Shapiro heterostructures discussed in the text.

	CB	VB
RS-I		−0.015
		−0.060
		−0.080
	1.695	−0.130
	1.630	−0.165
RS-II	1.695	0.003
	1.670	0.001
	1.660	−0.001
	1.630	−0.005
	1.610	−0.006
	1.585	−0.010
	1.580	−0.015
	1.555	−0.019
	1.540	−0.021
	1.530	−0.031

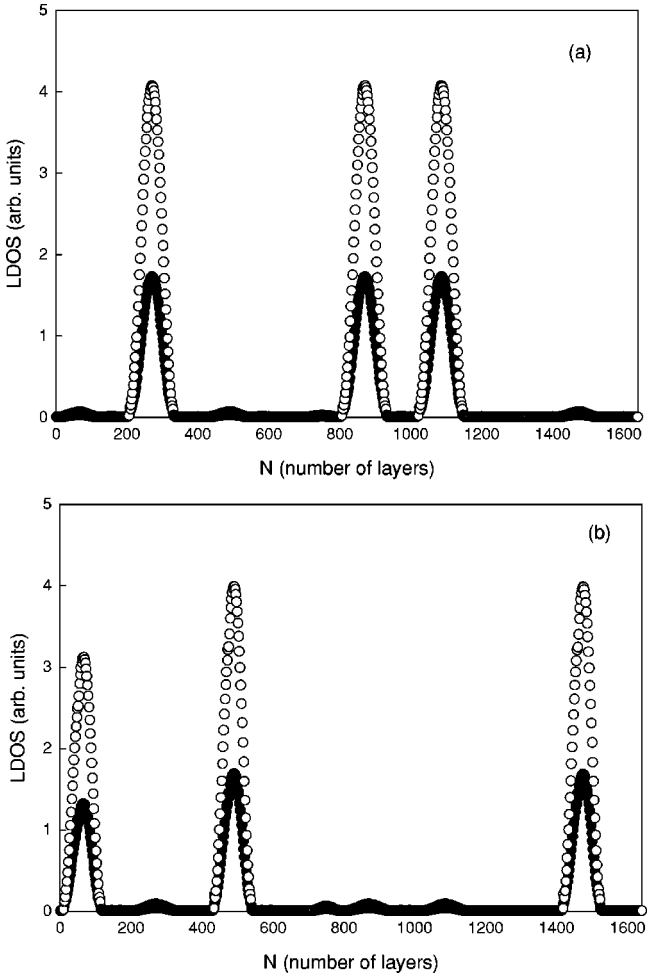

FIG. 5. Same as in Fig. 1 for the sixth generation of the RS-II system.

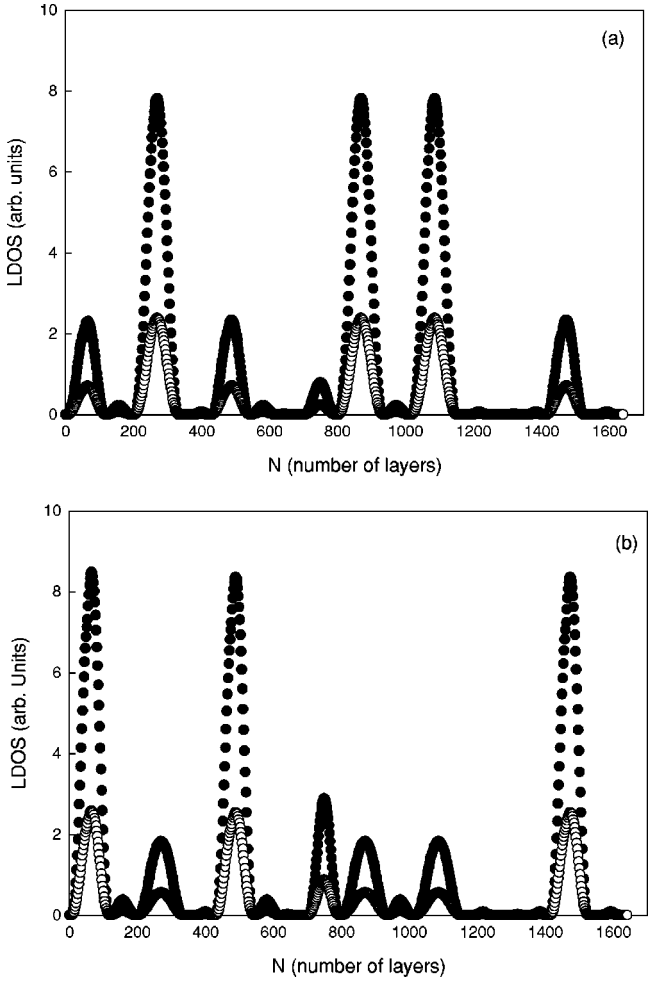

FIG. 6. Same as in Fig. 2 for the sixth generation of the RS-II system.

V. RUDIN-SHAPIRO HETEROSTRUCTURES

Here the stacking is recursive along the *z* direction with four generators, blocks *A, B, C,* and *D,* mapping the mathematical rule in the Rudin-Shapiro sequence, which is obtained from the letters *A, B, C, D* via the following substitution rules[42]

$$A \rightarrow AC, \quad B \rightarrow DC, \quad C \rightarrow AB, \quad D \rightarrow DB; \tag{4}$$

thus giving the following sequence:

$$S_0 = \{A\}, S_1 = \{AC\}, S_2 = \{ACAB\}, S_3 = \{ACABACDC\}, \ldots . \tag{5}$$

As in the Thue-Morse sequence, the number of terms in the sequence goes as 2^n. The *A* and *B* blocks are the same as in the previous cases, for both I and II cases (we shall denote these systems as RS I and RS II, respectively). On the other hand in the RS-I case the *C* block has 8 GaAs layers and 20 AlAs layers, whereas the *D* block has 8 GaAs layers and 10 AlAs layers. In the RS-II case the *C* block has 10 GaAs layers and the *D* block has 10 AlAs layers.

We present here results for the fifth RS-I generation, and the sixth RS-II generation, both having 64 slabs of AlAs and GaAs layers. The RS-I structure will have a repetition of the constituent 8-, 10- and 20-GaAs-layer quantum wells. On the other hand the RS-II structure due to the presence of the *C, A, AC, ACA,* and *CACA* blocks will have quantum wells of 10, 20, 30, 50, and 60 GaAs layers, respectively, thus introducing a richer variety in the heterostructure than in the former cases.

In Table V we present the lower conduction and higher valence states of the 8-, 30-, 50-, and 60-GaAs-layer isolated quantum wells.

In Table VI we present the lower conduction and higher valence states of the RS-I fifth generation and RS-II sixth generation. It is easy to see that the RS-I generation gives more or less the same results seen in Tables II and IV for the Fibonacci and Thue-Morse structures, respectively. On the other hand the RS-II structure presents a different kind of spectrum, due to the presence of the combination of the *A* and *C* blocks discussed above. Nevertheless, it is easy to see that the different states have energies very close to those of the states in the isolated quantum wells given in Tables I and V.

The LDOS for the different states in these structures can provide further evidence on their origin. Figure 5 gives the LDOS in the different layers of the RS-II structure together

with that of six neighboring AlAs layers to the left and right of the quasiperiodic structure, corresponding to the two lowest conduction states. In Fig. 5(a) we see the localization in the three wells having 60 GaAs layers. In Fig. 5(b) the localization is seen in the three wells with 50 GaAs layers. In Fig. 6 we present the same information for the two highest valence states. The picture is the same as in Fig. 5. In both cases we can see a lower spectral strength in the other wells, due to the closeness in energy of both states.

It is then clear that the RS-I heterostructure gives the same picture than that seen for the Fibonacci and Thue-Morse-type-I heterostructures. The RS-II heterostructure gives a different spectrum, due to the bigger richness of quantum well thicknesses, although the origin of the different states can be tied to the different isolated wells, as in all the other heterostructures considered here.

VI. CONCLUSIONS

We have studied the lowest conduction and highest valence states in different AlAs-GaAs heterostructures following the Fibonacci, Thue-Morse, and Rudin-Shapiro sequences, similar to those grown experimentally. We have considered different ways to form the material blocks entering the above sequences. It has been found that the Fibonacci, Thue-Morse, and Rudin-Shapiro-type-I heterostructures, having always in each block a barrier and well structure, have almost the same energy values. On the other hand the Rudin-Shapiro-type-II heterostructures exhibit different energy values coming from the bigger variety of GaAs wells forming the heterostructure. No spectrum fragmentation has been found in the energy ranges considered here for the different heterostructures. The different energy states can be adscribed to those of the different isolated quantum wells, not only by their numerical values, but also due to their spatial localization in the corresponding wells forming the quasiperiodic heterostructures. Heterostructures obtained by the periodic repetition of the constituent blocks give states with almost no difference in the energy and spatial localization as compared to those of the quasiperiodic systems. As an additional check we have studied a heterostructure containing an enlarged well in between two finite Fibonacci generations. The electronic states thus obtained would agree well with the PL transitions measured in a similar system.

It is thus clear that the electronic spectrum of real AlAs-GaAs finite quasiperiodic heterostructures does not exhibit the characteristic fragmentation seen in simple one-dimensional models. The different states come from those of the constituent wells in the structure.

The Rudin-Shapiro II systems provide an interesting way of producing a heterostructure with a fairly varied system of quantum wells, not possible in other simpler sequences.

ACKNOWLEDGMENT

This work was partially supported by the Ministerio de Ciencia y Tecnología (Spain) under Grant No. BFM2000-1330.

[1] D. Levine and P. J. Steinhardt, Phys. Rev. Lett. **53**, 2477 (1984).
[2] R. Merlin, K. Bajema, R. Clarke, F.-Y. Juang, and P. K. Bhattacharya, Phys. Rev. Lett. **55**, 1768 (1985).
[3] J. Todd, R. Merlin, R. Clarke, K. M. Mohanty, and J. D. Ax, Phys. Rev. Lett. **57**, 1157 (1986).
[4] R. Merlin, K. Bajema, J. Nagle, and K. Ploog, J. Phys. (France) **48**, C5–503 (1987).
[5] D. Shechtman, I. Blech, D. Gratias, and J. W. Cahn, Phys. Rev. Lett. **53**, 1951 (1984).
[6] A. I. Goldman and R. F. Kelton, Rev. Mod. Phys. **65**, 213 (1993).
[7] M. Kohmoto, L. P. Kadanoff, and C. Tang, Phys. Rev. Lett. **50**, 1870 (1983).
[8] M. Kohmoto and J. R. Benavar, Phys. Rev. B **34**, 563 (1986).
[9] M. Kohmoto, B. Sutherland, and C. Tang, Phys. Rev. B **35**, 1020 (1987).
[10] S. Ostlund, R. Pandit, D. Rand, H. J. Schellnhuber, and E. D. Siggia, Phys. Rev. Lett. **50**, 1873 (1983).
[11] S. Ostlund and R. Pandit, Phys. Rev. Lett. **29**, 1394 (1984).
[12] S.-R. Eric and S. Das Sarma, Phys. Rev. B **37**, 4007 (1988).
[13] Q. Niu and F. Nori, Phys. Rev. Lett. **57**, 2057 (1986).
[14] Q. Niu and F. Nori, Phys. Rev. B **42**, 10 329 (1990).
[15] Y. Liu and R. Riklund, Phys. Rev. B **35**, 6034 (1987).
[16] M. Fujita and K. Machida, Solid State Commun. **59**, 61 (1986).
[17] A. Süttö, J. Stat. Phys. **56**, 525 (1989).
[18] A. A. Yamaguchi, T. Saiki, T. Tada, T. Minomiya, K. Misawa, and T. Kobayashi, Solid State Commun. **85**, 223 (1993).
[19] D. Toet, M. Potemski, Y. Y. Wang, J. C. Maan, L. Tapfer, and K. Ploog, Phys. Rev. Lett. **66**, 2128 (1991).
[20] D. Munzar, L. Bročáev, J. Humlíček, and K. Ploog, J. Phys.: Condens. Matter **6**, 4107 (1994).
[21] A. Bovier and J. M. Ghez, J. Phys. A **28**, 2313 (1995).
[22] F. Domínguez-Adame and E. Maciá, Phys. Rev. B **53**, 13 921 (1996).
[23] E. Maciá and F. Domínguez-Adame, Phys. Rev. Lett. **76**, 2957 (1996).
[24] E. Maciá and F. Domínguez-Adame, Semicond. Sci. Technol. **11**, 1041 (1996).
[25] E. Maciá, Phys. Rev. B **60**, 10 032 (1999).
[26] E. Maciá and F. Domínguez-Adame, *Electrons, Phonons and Excitons in Low Dimensional Aperiodic Systems* (Editorial Complutense, Madrid, 2000).
[27] R. Pérez-Álvarez and F. García-Moliner, in *Contemporary Problems of Condensed Matter Physics*, edited by S. Vlaev and L. M. Gaggero-Sager (Nova Science, New York, 2001), p. 1.
[28] K. Hirose, D. Y. K. Ho, and H. Kamimura, J. Phys.: Condens. Matter **4**, 5947 (1992).
[29] J. Arriaga and V. R. Velasco, Physica A **241**, 377 (1997).
[30] J. Arriaga and V. R. Velasco, J. Phys.: Condens. Matter **9**, 8031 (1997).
[31] R. Pérez-Álvarez, F. García-Moliner, and V. R. Velasco, J. Phys.: Condens. Matter **13**, 3689 (2001).
[32] P. Vogl, H. P. Hjalmarson and J. D. Dow, J. Phys. Chem. Solids **44**, 365 (1983).

[33] D. J. Chadi, Phys. Rev. B **16**, 790 (1977).
[34] J. Arriaga, G. Armelles, M. C. Muñoz, J. M. Rodríguez, P. Castrillo, M. Recio, V. R. Velasco, F. Briones, and F. García-Moliner, Phys. Rev. B **43**, 2050 (1991).
[35] G. Armelles and V. R. Velasco, Phys. Rev. B **54**, 16 428 (1996).
[36] Y. Fu and K. A. Chao, Phys. Rev. B **43**, 4119 (1991).
[37] R. T. Kopf, M. H. Herman, M. L. Schnoes, and C. Colvard, J. Vac. Sci. Technol. B **11**, 813 (1993).
[38] F. García-Moliner and V. R. Velasco, *Theory of Single and Multiple Interfaces* (World Scientific, Singapore, 1992).
[39] L. Fernández-Alvarez, G. Monsivais, S. Vlaev, and V. R. Velasco, Surf. Sci. **369**, 367 (1996).
[40] A. A. Yamaguchi, T. Saiki, T. Tada, T. Minomiya, K. Misawa, T. Kobayashi, M. Kuwata-Gonokami, and T. Yao, Solid State Commun. **75**, 955 (1990).
[41] A. Thue, Norske Vididensk. Selsk. Skr. I., **7**, 1 (1906); M. Morse, Trans. Am. Math. Soc. **22**, 84 (1921).
[42] W. Rudin, Proc. Am. Math. Soc. **10**, 855 (1959); H. S. Shapiro, M.I.T. Master's thesis, Cambridge, MA (1951).